Supplementary Information for:

"Aqueous benzene-diols react with an organic triplet excited state and hydroxyl radical to form secondary organic aerosol"

Jeremy D. Smith[a,b], Haley Kinney[a], and Cort Anastasio[a,b]*

[a]Department of Land, Air and Water Resources, University of California – Davis, 1 Shields Ave., Davis, CA USA

[b]Agricultural and Environmental Chemistry Graduate Group, University of California - Davis, 1 Shields Ave., Davis, CA USA

Submitted to Physical Chemistry Chemical Physics

* Corresponding Author: Department of Land, Air and Water Resources, University of California, 1 Shields Ave., Davis, CA 95616, USA. Tel.: 530-754-6095; fax: 530-752-1552. E-mail address: canastasio@ucdavis.edu

This supporting information contains: 9 figures, 4 tables and 5 sections.

26

27 Table S1: Second-order rate constants of probe compounds reacting with •OH

	$k_{Probe+\bullet OH}$ (10^9 M^{-1} s^{-1})	Source
Phenol (pH 2)	1.91	Hermann et al.[1] ; Monod et al.[2]
Guaiacol (pH 6)	20	Buxton et al. [3]
Benzoate	6.0	Ashton et al.[4]
Benzoic Acid	5.9	Wander et al. [5]
Benzene (pH 3.5)	7.6	Kochany et al.[6]

28

29

30

31

32

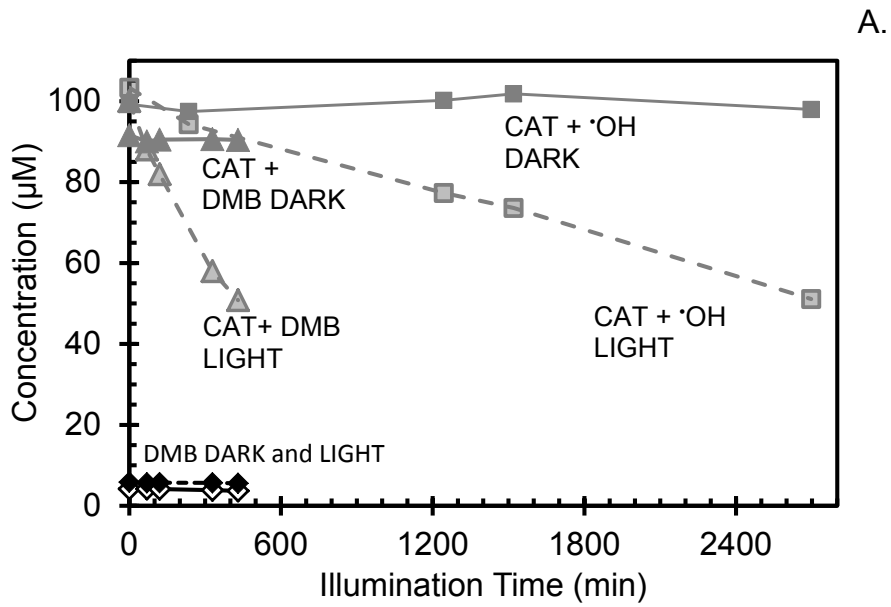

33

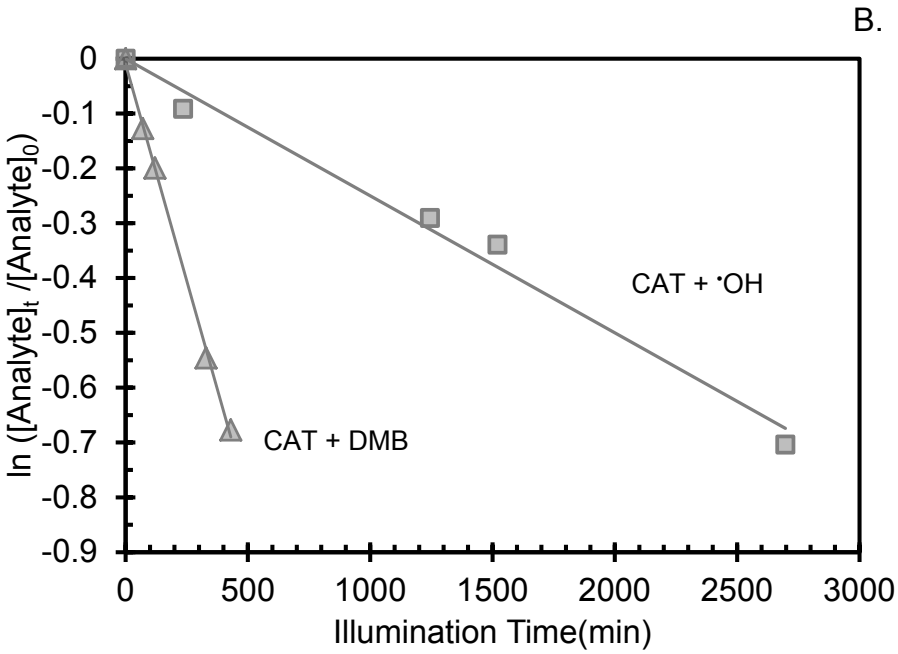

34

35 Figure S1: Panel A are representative decay curves for benzene-diol oxidation, and panel B are
36 the natural log transformation of the illuminated solutions in panel B. As there is not change in
37 concentration, DMB and dark control data are not included in panel B Data for $^3C^*$ oxidation is
38 with 100 μM catechol (CAT; triangles) and 5 μM 3,4-dimethoxybenzaldehyde (DMB;
39 diamonds) at pH 5. Data for •OH oxidation (squares) is 100 μM CAT with 100 μM HOOH
40 added as a •OH precursor at pH 5.

Section S1: Correction of pH 5 kinetic data to account for contributions from the protonated triplet excited state (HT)

The reactivity of benzene-diols with 3,4-dimethoxybenzaldehyde (DMB) is pH dependent. This behavior was seen in our previous work and we use a similar approach in this study to correct the pH 5 data for the contribution of the protonated DMB triplet.[7] The apparent first-order destruction rate constants for a phenol by the protonated and neutral triplet states of DMB are defined as k'_{HT} and k'_{T}, respectively. The value of k'_{HT} is larger than k'_{T} and thus our measured values of k'_{ArOH} (the observed rate constants for ArOH loss) at pH 2 are essentially equal to k'_{HT} (the first-order rate constant for ArOH with the protonated triplet). At pH 5, 98% of the triplet excited state of DMB should be in the neutral form (since the pK$_a$ for the triplet is 3.3[7, 8]). However, since the protonated triplet can be much more reactive than the neutral triplet (i.e., $k'_{HT} > k'_{T}$), in the pH 5 solutions we corrected for contribution of the protonated triplet excited state in our calculation of k'_{T} by using a modified form of Equation 4:

$$k'_{T} = \frac{(k'_{ArOH} - \alpha_{HT} \times k'_{HT})}{\alpha_{T}} \qquad [S8]$$

Here k'_{ArOH} is the apparent, photon-flux-normalized, measured first-order rate constant for phenol loss at pH 5 (Equations 2 and 3 in the main text) and α_{HT} and α_{T} are the mole fractions of the protonated and neutral triplet excited states, respectively. As seen in Table S2, the corrections for the pH 5 benzene-diol experiments are smallest for resorcinol (average correction = 1 %), intermediate for hydroquinone (average correction = 15%) and highest for catechol (average correction = 21%).

Table S2: Summary of k'_T correction in the pH 5 data due to the contribution from the protonated triplet (k'_{HT}).

Catechol				Resorcinol				Hydroquinone			
Concentration (μM)	**k'_{ArOH} (min^{-1})**	**k'_T (min^{-1})**	**% Difference**	**Concentration (μM)**	**k'_{ArOH} (min^{-1})**	**k'_T (min^{-1})**	**% Difference**	**Concentration (μM)**	**k'_{ArOH} (min^{-1})**	**k'_T (min^{-1})**	**% Difference**
100	1.04E-03	8.36E-04	22	100	9.30E-04	9.12E-04	2	100	7.66E-04	6.54E-04	16
100	9.82E-04	8.16E-04	18	100	9.40E-04	9.17E-04	2	100	5.76E-04	4.32E-04	28
50	1.49E-03	1.01E-03	38	100	1.27E-03	1.26E-03	1	100	8.15E-04	6.85E-04	17
50	1.07E-03	9.31E-04	14	50	1.56E-03	1.54E-03	1	100	5.69E-04	4.45E-04	25
50	1.50E-03	1.11E-03	30	50	1.27E-03	1.26E-03	1	100	7.69E-04	7.10E-04	8
50	1.51E-03	1.23E-03	21	30	2.38E-03	2.34E-03	2	50	1.20E-03	1.06E-03	2
30	1.56E-03	1.32E-03	17	30	2.15E-03	2.13E-03	1	30	1.84E-03	1.70E-03	8
30	9.73E-04	6.68E-04	37	30	1.72E-03	1.70E-03	1	10	2.98E-03	2.72E-03	9
10	2.27E-03	1.89E-03	18	10	2.76E-03	2.76E-03	< 1	5	4.39E-03	4.05E-03	8
10	2.65E-03	2.27E-03	15	10	2.00E-03	1.99E-03	< 1				
10	1.84E-03	1.49E-03	21	5	2.38E-03	2.38E-03	< 1				
5	2.32E-03	2.05E-03	12	5	2.77E-03	2.76E-03	< 1				
5	2.37E-03	2.12E-03	11								

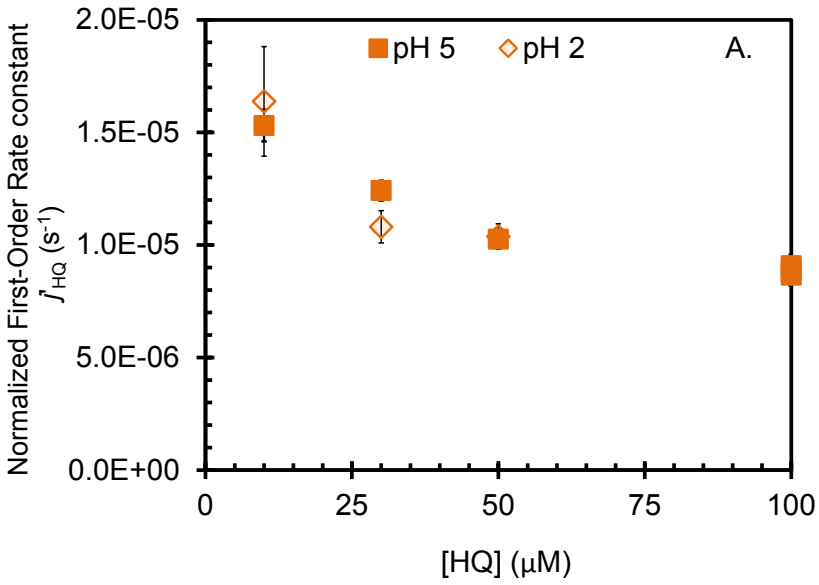

75

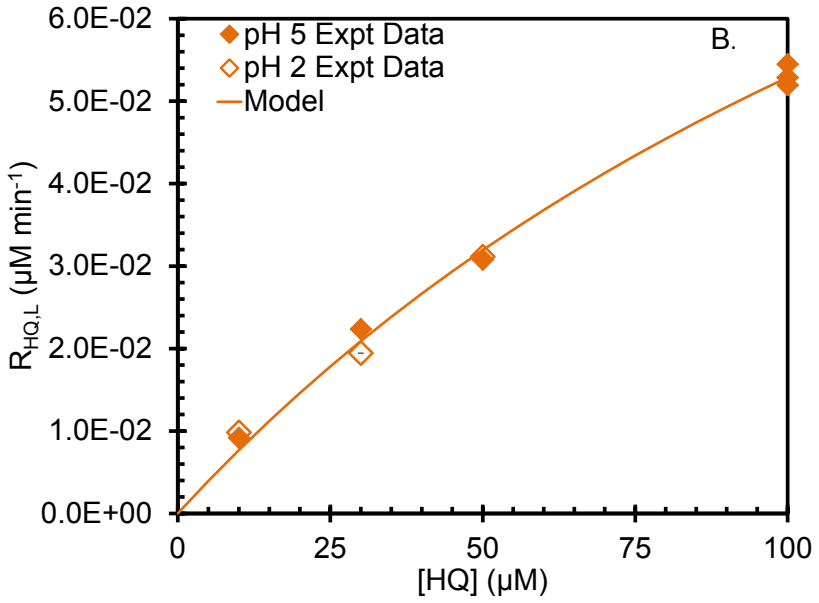

76

77 Figure S2: Direct photodegradation of hydroquinone (HQ) as a function of initial [HQ] at pH 2
78 (open orange diamonds) and pH 5 (filled orange diamonds). Panel A is the normalized first-
79 order rate constant for HQ loss and panel B is the rate of HQ loss as a function of concentration.
80 The line in Panel B is the non-linear regression fit to the data described in Section S1 (Equation
81 S6-S7) (R^2 = 0.88).

82

83

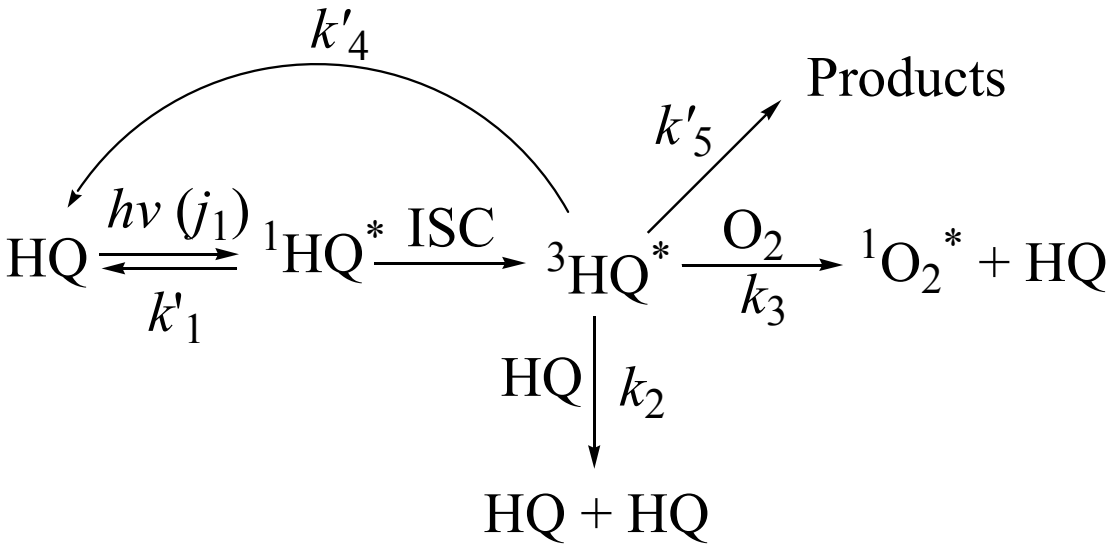

84

85

86 Figure S3: Proposed mechanism for the direct photodegradation of hydroquinone (HQ). ISC
87 represents the intersystem crossing from the first excited singlet state of HQ (^{1}HQ*) to the triplet
88 excited state of HQ. Based on previous work,[9] the k'_4 pathway is negligible.

89

90

91

92

93

94

95

96

97

98

99

Section S2: Hydroquinone Direct Photodegradation

The chemistry of hydroquinone (HQ) in sulfuric acid solutions (pH 4) under 313 nm light was investigated in previous work.[9] It was identified that ground state HQ rapidly forms a singlet excited state, followed by conversion to an excited triplet excited state (^{3}HQ*) with an intersystem crossing yield (ϕ_{ISC}) of 0.63. This system is shown in Figure S3. Based on this set of reactions, we can define the rate of change of the triplet excited state concentration (d[^{3}HQ*]/dt) as:

$$d[^3HQ^*]/dt = j_1\varphi_{ISC}[HQ] - k_2[HQ][^3HQ^*] - k_3[O_2][^3HQ^*] - k'_4[^3HQ^*] - k'_5[^3HQ^*] \quad \text{(S1)}$$

Where j_1 is the first-order rate constant for light absorption by HQ under our conditions, ϕ_{ISC} is the intersystem crossing efficiency of singlet HQ to triplet HQ, k_2 is the bimolecular rate constant for the quenching of ^{3}HQ* by ground state HQ, k_3 is the bimolecular rate constant for the reaction of molecular oxygen with ^{3}HQ* resulting in singlet oxygen, k'_4 is the first-order rate constant for relaxation of ^{3}HQ* to the ground state and k'_5 is a first-order process that results in the destruction of HQ. Since we do not know details about the k'_5 pathway resulting in the destruction of HQ, we have simply modeled it with respect to HQ loss. All rate constants correspond to those shown in Figure S3. If we assume a steady state of ^{3}HQ* in our system we can simplify Equation S1 to:

$$[^3HQ*] = \frac{j_1\varphi_{ISC}[HQ]}{k_2[HQ] + k_3[O_2] + k'_4 + k'_5} \quad \text{(S2)}$$

Since the relaxation of the triplet excited state back to the ground state (k'_4) is slow relative to the other processes,[9] Equation S2 then simplifies to:

$$[^3HQ*] = \frac{j_1\varphi_{ISC}[HQ]}{k_2[HQ] + k_3[O_2] + k'_5} \quad \text{(S3)}$$

The only term in Equation S3 that results in the loss of HQ is k'_5. Thus the observed rate of loss of HQ is:

$$R_{HQ,L} = k'_5[^3HQ*] \quad \text{(S4)}$$

Substituting Equation S3 into S4 we get:

$$R_{HQ,L} = k'_5\left(\frac{j_1\varphi_{ISC}[HQ]}{k_2[HQ] + k_3[O_2] + k'_5}\right) \qquad (S5)$$

We can rearrange this equation as:

$$R_{HQ,L} = \frac{1}{\left(\frac{k_2}{k'_5 j_1\varphi_{ISC}} + \frac{k_3[O_2] + k'_5}{k'_5 j_1\varphi_{ISC}} \times \frac{1}{[HQ]}\right)} \qquad (S6)$$

We fit our experimental data to Equation S6 using SigmaPlot Version 11 and the following regression form:

$$R_{HQ,L} = \frac{1}{a + \frac{b}{x}} \qquad (S7)$$

As shown in Figure S2, there is no pH dependence on direct photodegradation of HQ; thus we performed the regression using both pH 2 and pH 5 data. Using the molar absorptivities of HQ[10] and the measured photon flux of our illumination system,[7] we calculate that $j_1 = 4.14 \times 10^{-7}$ s^{-1}. The resulting '*a*' and '*b*' regression terms from our fit are 6.5 (±0.8) s μM^{-1}and 1.24 (±0.07) $\times 10^3$ s, respectively. The corresponding regression line of this fit is shown as the line in Figure S2B. We next use the values for $k_3[O_2]$ and $j_1\phi_{ISC}$ described in the main text (Section 3.1) to calculate the relative importance of the pathways for ^{3}HQ* loss. Since the k_2 pathway involves HQ, the relative importance of the pathways depends upon [HQ]. At 10 μM HQ, the relative sizes of k_2[HQ]: $k_3[O_2]$: k'_5 are 0.0305 s^{-1}: 5.81×10^5 s^{-1} : 1.80×10^3 s^{-1}, i.e,. <0.01 %, 99.7%, and 0.30% of the HQ triplet go down paths 2 (physical quenching by HQ), 3 (quenching with O_2), and 5 (product formation), respectively. Under aqueous conditions, pathway 4 (decay to the ground state) is negligible relative to other loss pathways.[9] In this system, the majority of HQ goes through non-destructive reaction with oxygen with only a very small fraction of triplet HQ destruction leading to products.

154

155 Table S3: Second-order rate constants for the non-reactive interactions between an ArOH and
156 ^{3}DMB*. Error bars are (±1 SE) calculated from the regression of Equation 3 in the main text.

157

	pH 2 k_Q (10^9 M^{-1} s^{-1})	pH 5 k_Q (10^9 M^{-1} s^{-1})
PhOH	1.6 (± 1.0)	14 (± 8)
GUA	1.7 (± 1.3)	1.0 (± 0.9)
SYR	2.6 (± 2.4)	0.3 (± 0.7)
CAT	3.1 (± 2.2)	14 (± 6)
RES	7.2 (± 3.5)	9.1 (± 3.6)
HQ	15 (± 7)	45 (± 17)

158

159

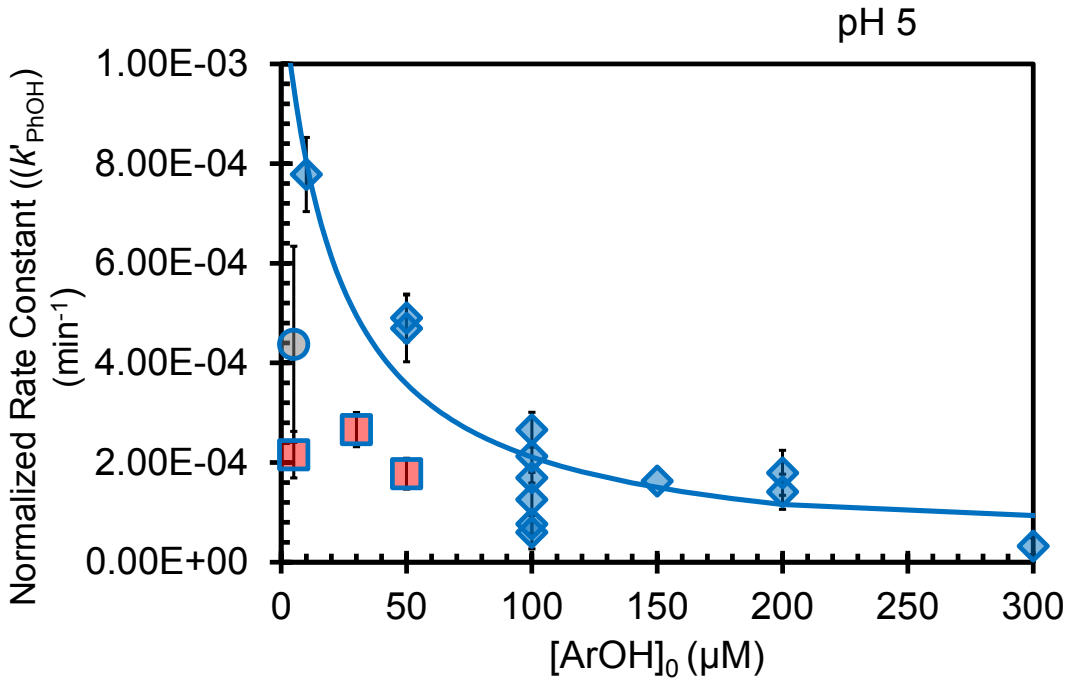

Figure S4: Dependence of phenol destruction kinetics on initial PhOH concentration at pH 5 in illuminated solutions containing 5 μM DMB (blue diamonds). Please see Smith et al.[7] for experimental information. All values have been normalized to Davis, CA Winter Solstice light conditions (j_{2NB}=0.0070 s^{-1}).[11] Error bars represent ±1 SE, propagated from the standard errors of k_{light} and j_{2NB}. The grey circle represents a data point (also at 5 μM DMB) that we removed from consideration due to noisy and non-linear kinetics for PhOH loss. The red squares represent results from three experiments with solutions containing 20 μM DMB; we removed these from the regression fit because of their different DMB condition. The blue diamonds were regressed to Equation 5 in the main text, yielding the parameters '*a*' = 856 min^{-1} and '*b*' =39 min μM^{-1}. In our previous work[7] we published this figure and fit the regression to all of the data points. The new regression fit (to just the blue diamonds) is shown in the figure above. The value for $k_{PhOH+3DMB*}$ determined from this fit (Table 2 in the main text) is in better agreement with the relative rate result for SYR and PhOH loss from illuminated DMB by Richards-Henderson et al:[12] the ratio $k_{SYR+3DMB*}/k_{PhOH+3DMB*}$ at pH 5 is 9.3 ± 3.1 from Richards-Henderson et al. and 12.1 ± 4.7 for our rate constants in Table 2.

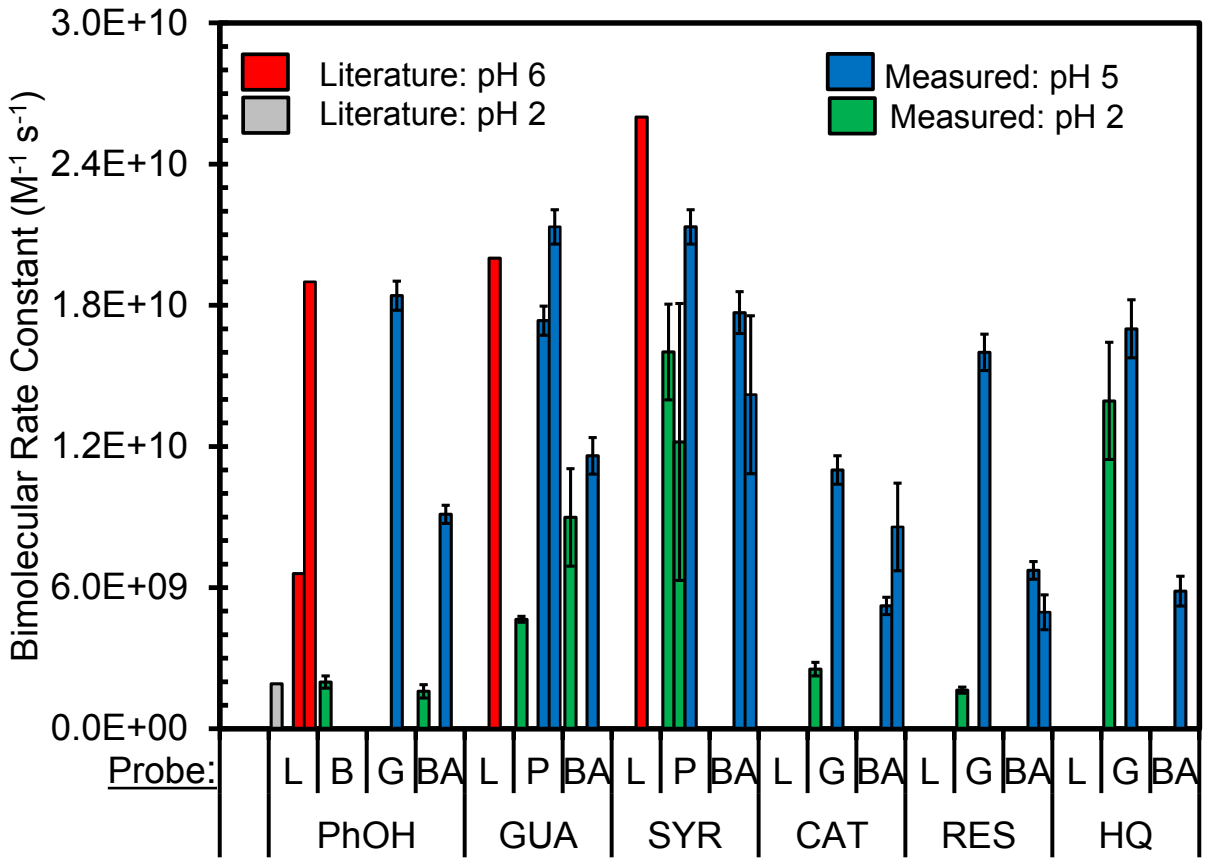

Figure S5: Summary of relative rate experiments for •OH reaction with phenols and benzenediols at pH 2 and 5. Each bar represents a single relative rate experiment using a given probe. Error bars represent the standard error of the slope (main text Equation 1). For each phenol there are three or four entries in the "Probe" row on the x-axis. The first entry (L) shows the literature value for the rate constant (Table S1). The values reported in Table 2 are the average of replicate experiments using different reference compounds shown here. The next two or three entries represent rate constants determined using different probes: B = benzene, G = guaiacol, BA = benzoic acid.

Section S3– Intersystem Crossing of DMB

Section S3.1: Determination of the DMB Intersystem Crossing Quantum Yield

In our previous work[7] we used data from Anastasio et al.[8] to estimate the intersystem crossing efficiency (ϕ_{ISC}) for 3,4-dimethoxybenzaldehyde (DMB) to go from the singlet excited state to triplet excited state. The value we estimated was 0.06±0.04; this intersystem crossing efficiency is important because it is needed to determine the second-order rate constants for ^{3}C* with phenols.[7] Given this importance, we experimentally determined the value in this work using new experiments.

In our previous work, we determined that the initial rate of phenol loss ($R_{ArOH,L}$) approaches a saturation plateau as phenol concentration increases.[7] Therefore, the y-intercept of a plot of the inverse of the initial rate of phenol loss ($R_{ArOH,L}^{-1}$) versus inverse phenol concentration ($[ArOH]^{-1}$) yields the rate of triplet formation, $R_{3C^*,F}$, at infinite phenol concentration, where essentially the fate of every triplet state is reaction with phenol and the phenol loss is the maximum possible value. At this saturation point, the rate of loss of phenol ($R_{ArOH,L,\infty}$) is equal to the rate of triplet excited state formation ($R_{3C^*,F}$) times the fraction of the triplet-phenol interactions that lead to a net reaction (loss) of phenol ($f_{Reaction}$):

$$R_{ArOH,L,\infty} = f_{Reaction} \times R_{3C*,F} \quad [S9]$$

We used syringol as our phenol in these experiments since it is very reactive and has a value of $f_{Reaction}$ that is essentially unity.[7] $R_{3C^*,F}$ is a function of the light-absorbing properties of DMB, the intensity of light, the concentration of DMB in our system, and the intersystem crossing efficiency. Thus at "infinite" phenol concentration, we can place the rate of triplet formation (Equation S4 in Smith et al.[7]into S9 above to express the loss of phenol as:

$$R_{ArOH,L,\infty} = 2.303 \times [DMB] \times l \times \varepsilon_{313nm,DMB} \times \varphi_{ISC} \times I'_{313nm} \quad [S10]$$

where l is the cell pathlength, $\varepsilon_{313nm,DMB}$ is the molar absorptivity of DMB at 313 nm (9155 ± 177 M^{-1} cm^{-1})[7] and I'_{313nm} is the actinic flux at 313 nm in our illumination system. (To determine ϕ_{ISC} we only illuminate our sample with 313 nm radiation to simplify the experiment.) Solving Equation S10 for ϕ_{ISC} yields:

$$\varphi_{ISC} = \frac{R_{ArOH,L,\infty}}{2.303 \times \varepsilon_{313nm,DMB} \times l \times I'_{313nm} \times [DMB]} \quad [S11]$$

where $R_{ArOH,L,\infty}$ is the maximum phenol loss possible, calculated as the y-intercept of the plot of $R_{ArOH,L}^{-1}$ vs. $[ArOH]^{-1}$, I'_{313nm} is calculated from j_{2NB}, the measured decay constant of the

chemical actinometer 2-nitrobenzaldehyde (2NB), which was measured on the day of each ϕ_{ISC} experiment:[11]

$$I'_{313nm} = \frac{j_{2NB}}{2.303 \times \varepsilon_{2NB,313nm} \times l \times \varphi_{2NB}} \quad \text{[S12]}$$

The term $\varepsilon_{313nm,2NB} \times \phi_{2NB}$ is the product of the molar absorptivity of 2NB at 313 nm and the quantum yield for destruction of 2NB (640 ± 44 L mol-photons^{-1} cm^{-1}).[7, 13]

Syringol (SYR) and DMB were used as the reactants in these experiments to determine ϕ_{ISC} of DMB.[7] SYR concentrations ranged from 5-200 μM with a constant [DMB] of 5 μM at pH 5. Results from our two new determinations of ϕ_{ISC} are shown in Figure S6. The difference between the two experiments performed can be explained in part by the difference in $j_{2NB,exp}$ for the two experiments, which were 0.0131 s^{-1} (Panel A) and 0.0194 s^{-1} (Panel B), corresponding to I'_{313nm} values of 8.9 ×10^{-6} and 1.3×10^{-5} mol photons L^{-1} cm^{-1}. Using Equation S11 the resulting ϕ_{ISC} values are 0.08 ± 0.01 and 0.12 ± 0.01 for Figures S6A and B, respectively, giving an average (± 1σ) value for ϕ_{ISC} of 0.10 ± 0.03.

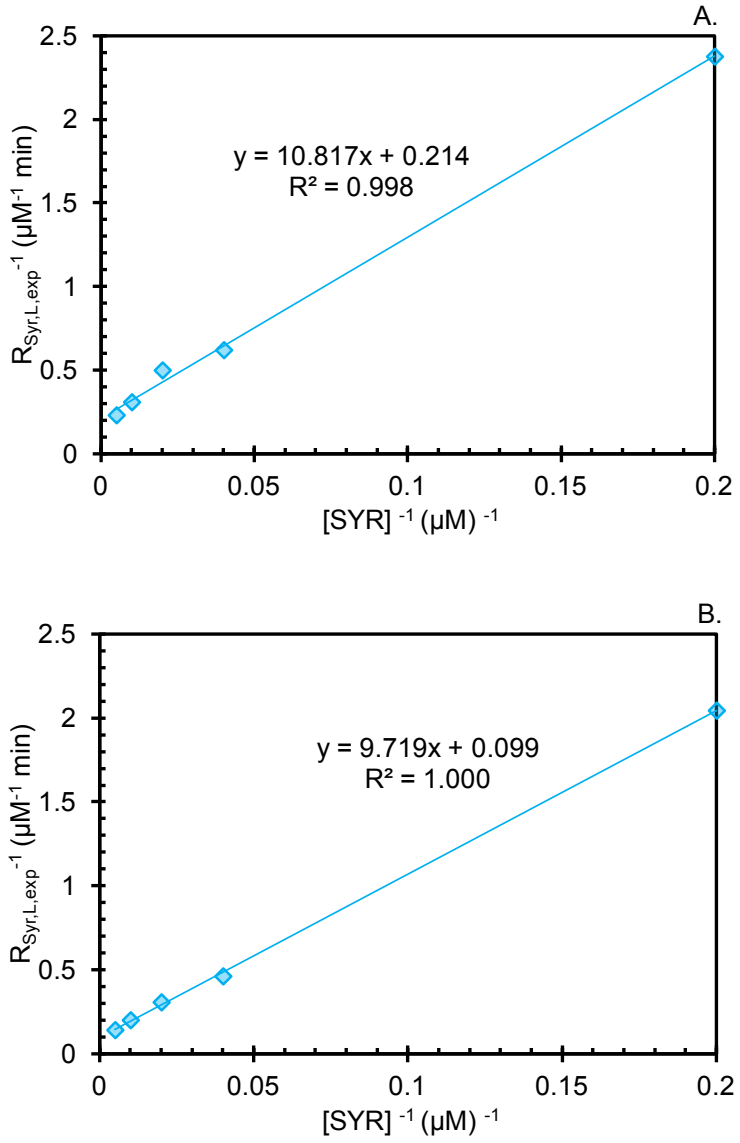

Figure S6: Experimental results of the loss of SYR from oxidation by the triplet excited state of DMB at 313 nm. Panels A and B are the inverse plots of the two independent experiments of SYR oxidation by ^{3}C* of DMB. The y-intercept of each panel is assumed to be the inverse of the maximum SYR loss at infinite [SYR] (Section S3).

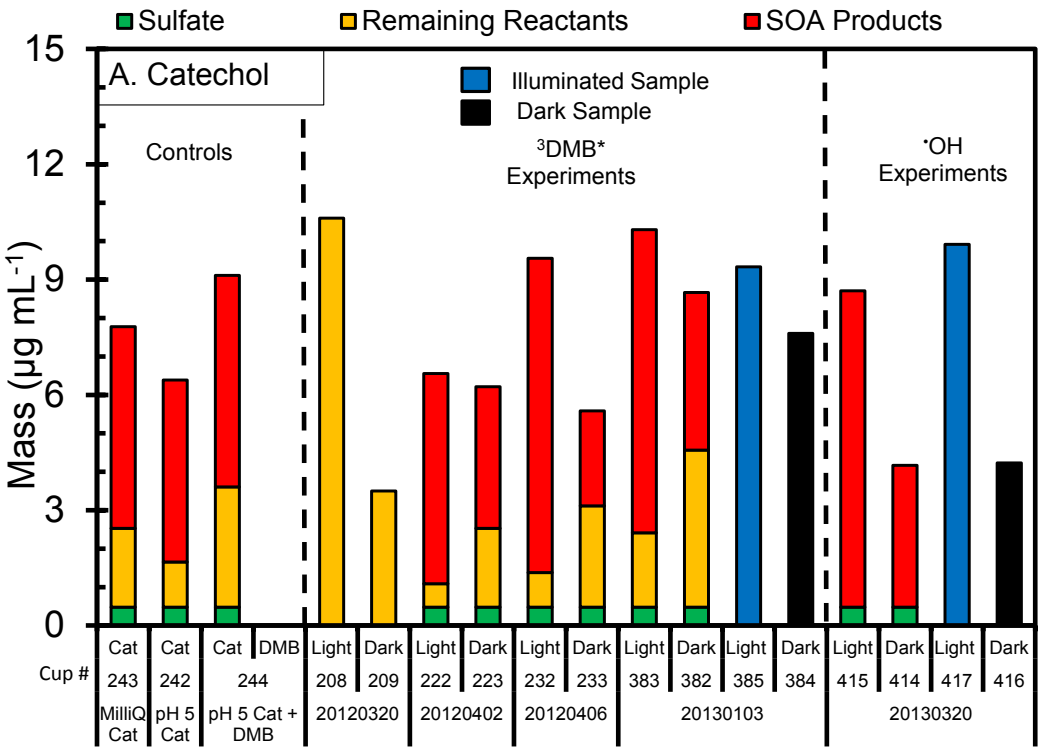
Sulfate
Remaining Reactants
SOA Products
A. Catechol
Illuminated Sample
Dark Sample
Controls
3DMB* Experiments
•OH Experiments
Mass (µg mL-1)
0
3
6
9
12
15
Cup #
Cat 243 MilliQ Cat
Cat 242 pH 5 Cat
Cat 244 pH 5 Cat + DMB
DMB
Light 208 Dark 209 20120320
Light 222 Dark 223 20120402
Light 232 Dark 233 20120406
Light 383 Dark 382 Light 385 Dark 384 20130103
Light 415 Dark 414 Light 417 Dark 416 20130320

247

248

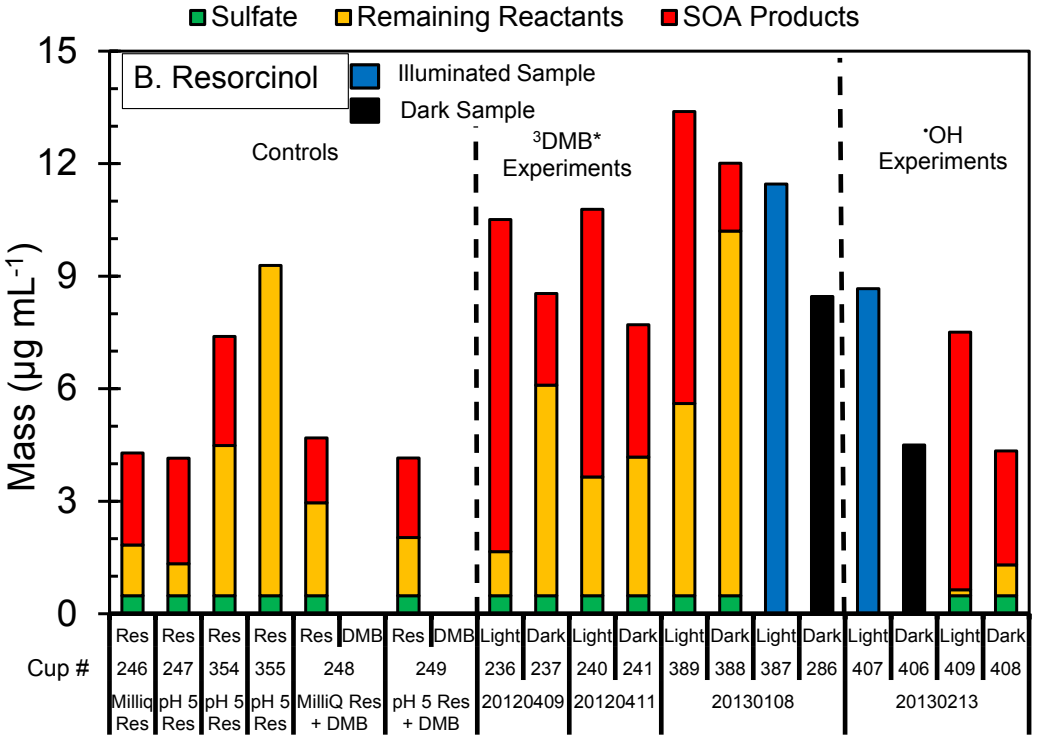
Sulfate
Remaining Reactants
SOA Products
B. Resorcinol
Illuminated Sample
Dark Sample
Controls
3DMB* Experiments
•OH Experiments
Mass (µg mL-1)
0
3
6
9
12
15
Cup #
Res 246 Milliq Res
Res 247 pH 5 Res
Res 354 pH 5 Res
Res 355 pH 5 Res
Res 248 MilliQ Res + DMB
DMB
Res 249 pH 5 Res + DMB
DMB
Light 236 Dark 237 20120409
Light 240 Dark 241 20120411
Light 389 Dark 388 Light 387 Dark 286 20130108
Light 407 Dark 406 Light 409 Dark 408 20130213

249

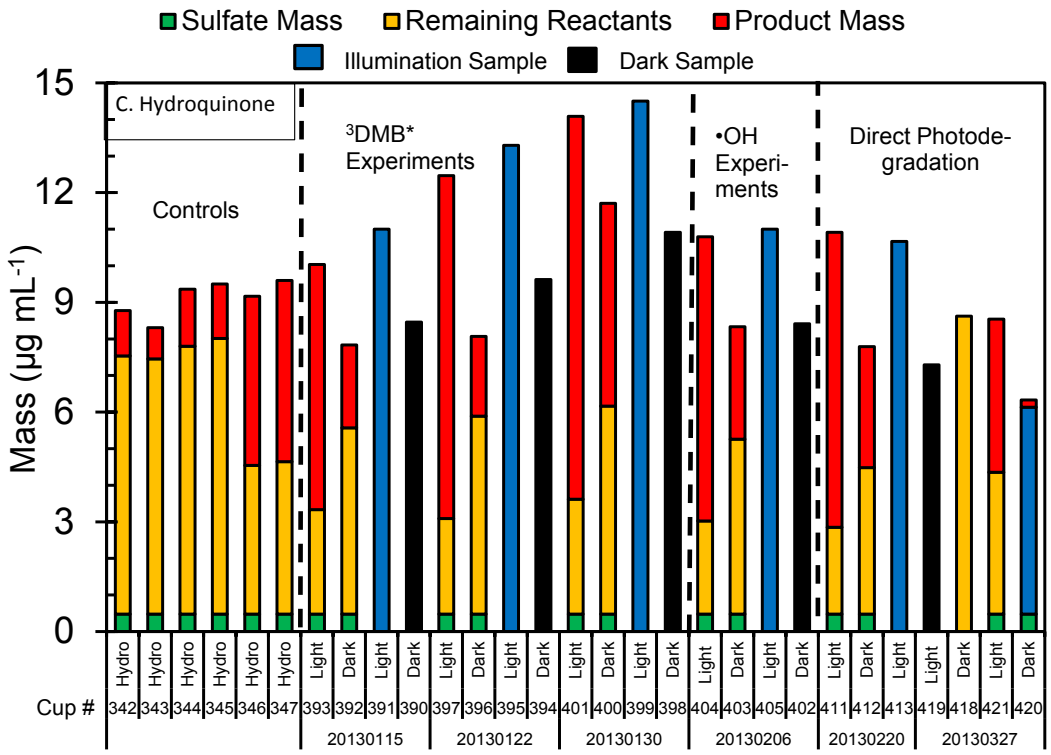

Figure S7: Masses in each blown-down solution for experiments with catechol (Panel A), resorcinol (Panel B), and hydroquinone (Panel C). Each illumination experiment is categorized by the sample ID as "YearMonthDay", i.e., the experiment performed on March 5, 2013 is listed as '20130315'. For the Control experiments (the first series of experiments in each graph) we prepared the solution and immediately blew it down with N_2. In all experiments (controls, illuminated and dark), only remaining diol mass was found in the cups and all DMB evaporated during blow down. In contrast, for the Dark Control accompanying each illumination (Light) experiment, we made the solution and it sat in the dark with the illuminated sample during the entire experiment. ^{3}DMB* illumination experiments contained 5 µM DMB as a precursor for the DMB triplet state, and OH experiments contained 100 µM HOOH as a precursor for OH. Direct photodegradation experiments for HQ only contained hydroquinone (HQ) and H_2SO_4. All experiments were performed at pH 5. The 'Cup #' refers to the individual cup that was blown down to determine the reported mass. For a subset of the cups we measured the amount of benzene-diol remaining in the blown-down material. For these cups (stacked bars) we show: the calculated sulfate mass (green portion; determined from the 5 µM H_2SO_4 added to the solution), the mass concentration of remaining benzene-diol (yellow portion), and the remaining mass, i.e., SOA products (red portion). In some cups we did not measure the concentrations of remaining reactants. In these cases a blue bar corresponds to the total cup mass concentration for the illuminated (light) sample and a black bar for the mass in the corresponding dark sample.

Section S4: Composition and kinetics for aqueous mixtures of phenols

Section S4.1: Phenol Concentrations

In this section we explain how we estimated the composition of the aqueous phenol mixtures (section 3.4 in main text) that we used to mimic the concentrations of some of the major phenols in ambient fog and cloud drops in areas with biomass burning. We first estimated the aqueous concentrations of phenols using wood-burning emissions data of Schauer et al.[14] and ambient phenol and particulate matter data for a wintertime stagnation event in Bakersfield or Fresno, California from Schauer and Cass.[15] The total concentration of an individual phenol, [ArOH(tot)] (μg m^{-3}), during this event was calculated as:

$$[ArOH(tot)] = [Primary\ OC\ mass] \times \frac{R_{ArOH,tot} \times 0.001\ g\ mg^{-1}}{R_{PM,fine} \times f_{OC}} \quad \text{(S12)}$$

where [Primary OC mass] is the primary organic carbon mass concentration from wood combustion reported by Schauer and Cass[15] based on CMB modeling for both hard and softwood burning during the Bakersfield (5.7 and 4.5 μg m^{-3}, respectively) and Fresno (8.7 and 17.5 μg m^{-3}, respectively) events, $R_{ArOH,tot}$ is the measured emission rate of the gas- and particulate phase phenol (mg phenol per kg wood burned) from a source profile,[14] $R_{PM,fine}$ is the measured emission rate of fine particulate matter (PM) from hard and softwood burning (5.1 and 9.5 g per kg wood burned, respectively)[14], and f_{OC} is the fraction of PM that is organic carbon (59 and 56 % for hardwood and softwood burning, respectively)[14]. For mixture experiments we lumped emissions into 4 classes: phenols (C_6H_5OH; PhOH), guaiacols, syringols, and *m,p*-benzene-diols. *o*-benzene-diol (catechol) was grouped with PhOH due to its similar reactivity and Henry's law constant. We took the measured phenols in Schauer and Cass[15] and assigned them to a phenol reactivity class based on their structures and their resemblance to PhOH, GUA, or SYR. A detailed description of this assignment is in an upcoming publication (Smith et al., 2015; *In preparation*). For SOA rate estimations we used data reported for catechol, resorcinol and hydroquinone individually.

Using [ArOH(tot)] we can then calculate the available gas-phase phenol concentration at the measured level of OA (26.2 μg m^{-3} for Fresno, CA)[15] using the saturation concentration of each phenol (C_i*) calculated using [16]:

$$C_i^* = \frac{p_{vap}^o}{RT} \times MW_i \quad \text{[S13]}$$

Where p^o_{vap} is the saturation vapor pressure (EPI Suite Version 4.1 (US EPA); values of 4.8×10^{-6}, 3.2×10^{-8}, and 6.4×10^{-7} atm for CAT, RES, and HQ, respectively), R is the ideal gas constant (0.0825 L atm mol^{-1} K^{-1}), T is temperature (all calculations at 5°C), and MW_i is the molecular weight of a given phenol. The fraction of a phenol that will be in the particulate phase ($f_{PM,i}$) can be estimated from:

$$f_{PM,i} = \frac{1}{1 + \frac{C_i^*}{[POA]}} \quad \text{[S14]}$$

After determining the gas-phase concentration of each phenol or phenol class, we allowed the phenols to partition into a hypothetical fog assuming Henry's law equilibrium. The phenols used in the work have moderate to high Henry's Law constants (K_H), with values of 1.5×10^4, 5.0×10^3, 2.5×10^4, 1.5×10^7 M atm^{-1}, for PhOH, GUA, SYR, and RES/HQ respectively.[17] For a typical foggy winter day in the Central Valley of California (pH 5, Liquid Water Content (L) = 1.0×10^{-7} L_{aq} L_g^{-1}, T = 278 K) we calculated the fraction of each phenol class that would exist in the aqueous phase (f_{aq}) as:

$$f_{aq} = \frac{1}{1 + \frac{1}{K_H \times L \times R \times T}} \quad \text{(S15)}$$

where R is the gas constant (0.08205 L atm mol^{-1} K^{-1}). The aqueous fraction for each phenol class, calculated assuming each member has the same K_H value as the class namesake (i.e., PhOH, GUA, SYR, and diols), is shown in Figure S9. Using this information we estimate the aqueous concentration of each phenol class ([ArOH(aq)]) reported by Schauer and Cass[15] as

$$[ArOH(aq)] = [ArOH]_{gas} \times f_{aq} \times MW_{ArOH}^{-1} \times \left(\frac{10^{-9} g\, m^3}{\mu g\, L}\right) \quad \text{(S16)}$$

where MW_{ArOH} is the molecular weight of the phenol class (assumed as phenol (C_6H_5OH), guaiacol, syringol, or catechol for the respective classes). The mole fraction of each phenol class to the total phenol concentration ($f_{ArOH,mix}$) was determined as:

$$f_{ArOH,mix} = \frac{[ArOH(aq)]_{class}}{[ArOH(aq)]_{total}} \quad \text{(S17)}$$

where $[ArOH(aq)]_{class}$ is the aqueous concentration of a given phenol class, and $[ArOH(aq)]_{total}$ is the sum of all phenol classes reported by Schauer and Cass[15]. We assumed an initial mixture concentration of 100 μM total aqueous phenol based on previous estimations,[8] and applied the corresponding class fraction to this initial value.

Section S4.2: Theoretical k'_{ArOH} Calculations

The rate of loss of phenol due to reaction with the triplet excited state of DMB is:

$$R_{ArOH,L} = k_{ArOH+3C*}[ArOH][^3DMB*] \quad \text{(S18)}$$

. If we assume ^{3}DMB* is at steady state, the equation can be rewritten in terms of a pseudo first-order rate constant:

$$R_{ArOH,L} = k'_{ArOH}[ArOH] \quad \text{(S19)}$$

where

$$k'_{ArOH} = k_{ArOH+3C*}[^3DMB*] \quad \text{(S20)}$$

Applying a steady-state approximation to the system we can calculate [^{3}DMB*] for a given experiment using Equation S19:

$$[^3DMB*] = \frac{R_{3DMB*,F}}{\sum(k_{ArOH+3DMB*} + k_Q)[ArOH] + k_{O2+3DMB*}[O_2] + k'_{3DMB*}} \quad \text{(S21)}$$

where $R_{3DMB*,F}$ is the rate of DMB triplet excited state formation under winter solstice sunlight in Davis ($R_{3DMB*,F} = j_{hv,abs}\,\phi_{ISC}$[DMB] =2.3 (± 0.5) μM min^{-1}; Section 3.1main text), $\Sigma(k_{ArOH+3DMB*} + k_Q)$ is the sum of all phenol sinks for ^{3}DMB*, $k_{O2+3DMB*}[O_2]$ is the reaction of the triplet with molecular oxygen, and k'_{3C*} is the relaxation of the triplet to the ground state. We have previously determined that ($k_{O2+3DMB*}[O_2] + k'_{3DMB*}$) = 5.8 ×10^5 s^{-1}.[7] Using our calculated value of [^{3}DMB*], Equations S18, and our second-order rate constants (Table 1 of the main text and Equation S18), we can predict k'_{ArOH} for each phenol in our illuminated HW and SW mixtures. Values of $k_{ArOH+3DMB*}$ were determined in this work (Table 1; main text) and in previous work.[7] Values of [^{3}DMB*] were 4.6 × 10^{-14} M, 4.2 × 10^{-14} M, 4.3× 10^{-14} M, 4.1 × 10^{-14} M for the (1) HW phenols (no diols), (2) SW phenols (no diols), (3) HW diols (no Phenol), and (4) SW diols (no Phenol) solutions, respectively.

Equation S21 is also used to estimate the [3DMB*] for individual phenol experiments shown in Figure 4 (main text). For experiments with initial concentrations of 1, 5, and 10 μM DMB (corresponding to the bottom, middle, and top lines of Figure 4A), we calculate triplet excited state concentrations of approximately 9 × 10^{-15}, 5 × 10^{-14}, and 9 × 10^{-14}, respectively in our hypothetical fog/cloud drops; these are in the range of the ^{3}C* concentration of 9 × 10^{-13} M that we recently estimated for a Davis fog water. [12]

Section S5: Empirical fit of •OH data as a function of pH

In order to estimate the importance of •OH across a wide range of solution acidities, we estimated values of $k_{ArOH+•OH}$ between pH 0 and 7 based on experimental results at pH 2 and 5, as well as a literature value of HQ at pH 6.5.[3] We did not include the available literature values[3] at pH 9 as these values were measured near the expected pK_a's of CAT, RES and HQ.[18] Since the phenolate ion contains a higher electron density in the aromatic ring we expect higher rate constants for solutions near, or above, the pKa values of phenols,[18] thus producing a system that is not comparable to that at pH 2 or 5.

For CAT and RES, we assume that $k_{ArOH+•OH}$ at pH < 2 is equal to our measured value at pH 2 and that values above pH 5 are equal to the measured pH 5 rate constants (Figure S8). In between pH 2 and 5 we use a linear regression, as shown in Figure S7. For HQ the experimental values at pH 2 and 5 were not statistically different (main text, Table 2), so we assume the average of these two values for pH < 5. For pH > 6.5 we assume the rate constant is equal to the literature value[3] at pH 6.5, and we use a linear regression between the pH 5 and 6.5 values (Figure S7). We stop our pH analysis at pH 7 to eliminate interference from the phenolate ion on our system.

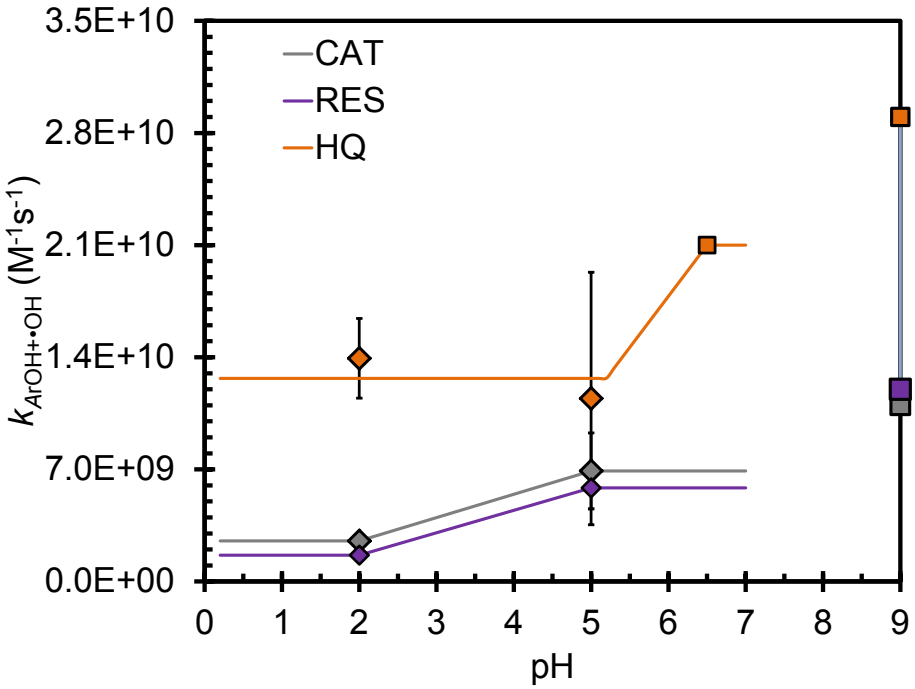

Figure S8: Estimated hydroxyl radical rate constants for catechol (CAT; grey), resorcinol (RES; purple), and hydroquinone (HQ; orange) as a function of pH. Diamond data points are experimentally determined values from this work, and square data points are literature values.[3] Rate constants at pH 9 were not included in our fits to the data because of the presence of the phenolate ion in these basic solutions.

380 Table S4: Compilation of reaction conditions and results for the mixture experiments.

Mixture	Initial Fraction[a] of $[ArOH]_{tot}$	Reaction Time (min)	% Loss	Calculated k'_{ArOH}/ Measured k'_{ArOH}
HW: No Diols		240		
PhOH	0.33		23	0.22
GUA	0.07		72	1.25
SYR	0.60		94	0.98
HW: No PhOH		240		
GUA	0.07		56	2.68
SYR	0.61		74	1.99
CAT	0.29		N/A[b]	N/A[b]
HQ	0.03		50	1.53
SW: No Diols		1305		
PhOH	0.79		40	0.73
GUA	0.21		100	1.06
SW: No PhOH		360		
GUA	0.06		19	8.76
CAT	0.88		32	1.81
HQ	0.06		79	0.80

381

382 [a] Total [ArOH] =100µM.
383 [b] CAT could not be quantified during experiments due to a co-eluting product peak formed from
384 SYR oxidation.
385

386

387

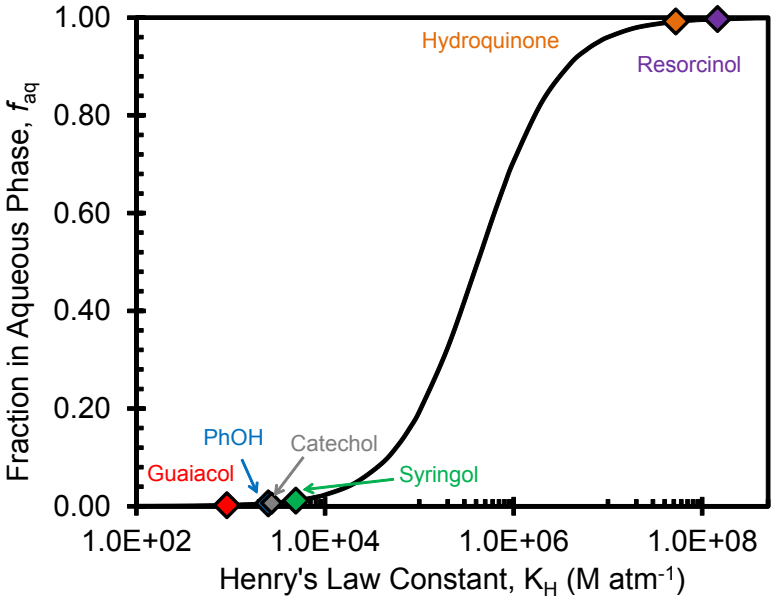

388

389 Figure S9: Fraction of a phenol in fog drops under typical California Central Valley fog
390 conditions: T =5 °C, LWC = 1.0×10^{-7} L_{aq} L_g^{-1}. Values were calculated using Equation S13.
391 Henry's Law constants were taken from Sander et al.[17]

392

393

394

395

396

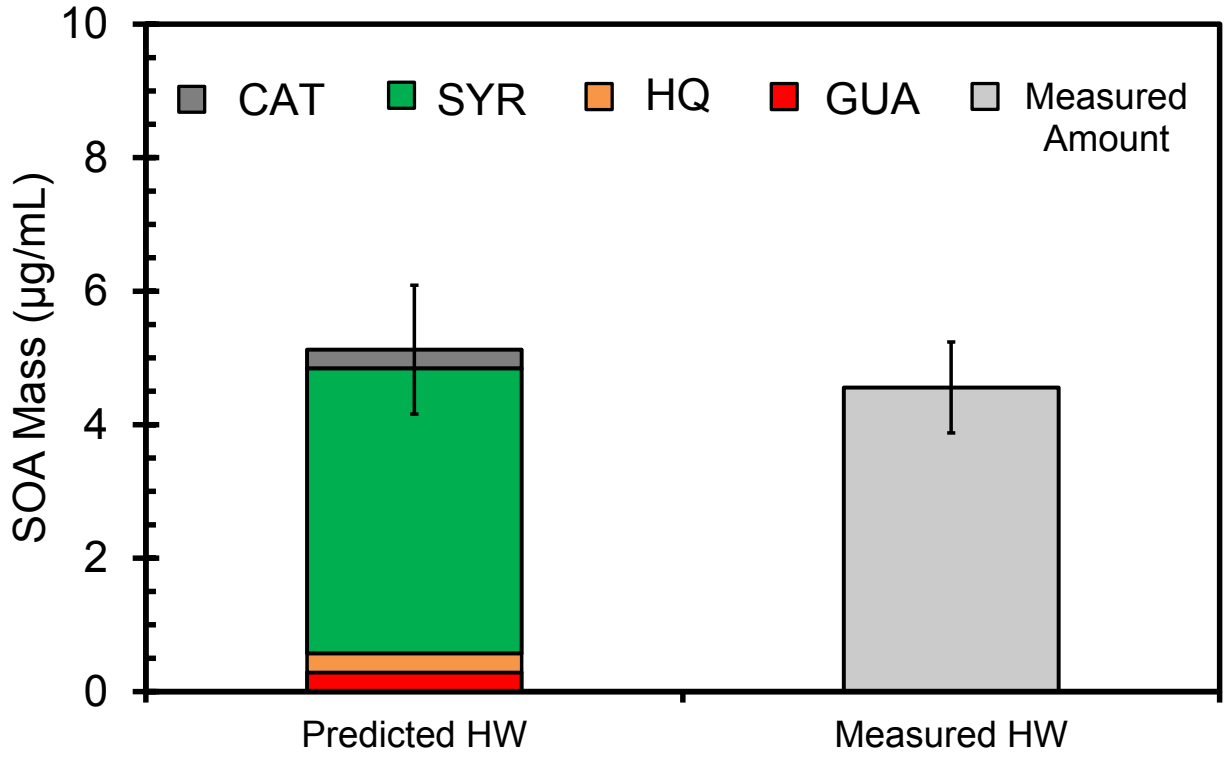

Figure S10: Comparison of predicted and measured SOA mass concentrations (corrected for the dark control mass concentration) for an illuminated hardwood mixture (no PhOH) containing benzene-diols and HOOH (i.e., oxidation by •OH). The initial concentrations of each phenol/benzene-diol in the mixture are shown in Figure 4 of the main text and Table S4. Error bars represent the propagated errors from each individual phenol/benzene-diol mass determination as shown in Section S3.

References

1. H. Herrmann, D. Hoffmann, T. Schaefer, P. Brauer and A. Tilgner, *ChemPhysChem*, 2010, **11**, 3796-3822.
2. A. Monod, L. Poulain, S. Grubert, D. Voisin and H. Wortham, *Atmospheric Environment*, 2005, **39**, 7667-7688.
3. G. V. Buxton, C. L. Greenstock, W. P. Helman and A. B. Ross, *Journal of Physical Chemistry Reference Data*, 1988, **17**, 513-886.
4. L. Ashton, G. V. Buxton and C. R. Stuart, *Journal of the Chemical Society, Faraday Transactions*, 1995, **91**, 1631-1633.

5. R. Wander, P. Neta and L. M. Dorfman, *Journal of Physical Chemistry*, 1968, **72**, 2946-2949.

6. J. Kochany and J. R. Bolton, *Environmental Science & Technology*, 1992, **26**, 262-265.

7. J. D. Smith, V. Sio, L. Yu, Q. Zhang and C. Anastasio, *Environmental Science & Technology*, 2014, **48**, 1049-1057.

8. C. Anastasio, B. C. Faust and C. J. Rao, *Environmental Science & Technology*, 1997, **31**, 218-232.

9. G. F. Vesley, *Journal of Physical Chemistry*, 1971, **75**, 1775-1781.

10. J. D. Smith, H. Kinney and C. Anastasio, *Atmospheric Environment*, 2014, In Preparation.

11. E. S. Galbavy, K. Ram and C. Anastasio, *Journal of Photochemistry and Photobiology A: Chemistry*, 2010, **209**, 186-192.

12. N. K. Richards-Henderson, A. T. Pham, B. B. Kirk and C. Anastasio, *Environmental Science & Technology*, 2014, DOI: 10.1021/es503656m.

13. C. Anastasio, B. C. Faust and J. M. Allen, *Journal of Geophysical Research*, 1994, **99**, 8231-8248.

14. J. J. Schauer, M. J. Kleeman, G. R. Cass and B. R. T. Simoneit, *Environmental Science & Technology*, 2001, **35**, 1716-1728.

15. J. J. Schauer and G. R. Cass, *Environmental Science & Technology*, 2000, **34**, 1821-1832.

16. M. Hallquist, J. C. Wenger, U. Baltensperger, Y. Rudich, D. Simpson, M. Claeys, J. Dommen, N. M. Donahue, C. George, A. H. Goldstein, J. F. Hamilton, H. Herrmann, T. Hoffmann, Y. Iinuma, M. Jang, M. E. Jenkin, J. L. Jimenez, A. Kiendler-Scharr, W. Maenhaut, G. McFiggans, T. F. Mentel, A. Monod, A. S. H. Prevot, J. H. Seinfeld, J. D. Surratt, R. Szmigielski and J. Wildt, *Atmospheric Chemistry and Physics*, 2009, **9**, 5155-5236.

17. R. Sander, http://www.henrys-law.org/, 1999.

18. P. G. Tratnyek and J. Holgne, *Environmental Science & Technology*, 1991, **25**, 1596-1604.